RSC Advances

This is an *Accepted Manuscript*, which has been through the Royal Society of Chemistry peer review process and has been accepted for publication.

Accepted Manuscripts are published online shortly after acceptance, before technical editing, formatting and proof reading. Using this free service, authors can make their results available to the community, in citable form, before we publish the edited article. This *Accepted Manuscript* will be replaced by the edited, formatted and paginated article as soon as this is available.

You can find more information about *Accepted Manuscripts* in the Information for Authors.

Please note that technical editing may introduce minor changes to the text and/or graphics, which may alter content. The journal's standard Terms & Conditions and the Ethical guidelines still apply. In no event shall the Royal Society of Chemistry be held responsible for any errors or omissions in this *Accepted Manuscript* or any consequences arising from the use of any information it contains.

ROYAL SOCIETY OF CHEMISTRY

www.rsc.org/advances

Phase Transition and Piezoelectric Properties of Alkali Niobate Ceramics through Composition Tuning

Yuanyu Wang,[a,b] Nuoxin Xu,[a] Qilong Zhang,[a,*] Hui Yang[a]

a School of Materials Science and Engineering, State Key Lab Silicon Mat, Zhejiang University, Hangzhou 310027, PR China

b College of Materials and Metallurgy, Guizhou University, Guiyang 550025, PR China

Abstract: (1-x)($K_{0.40}Na_{0.60}$)($Nb_{0.95}Sb_{0.05}$)O_3-x($Bi_{0.5}K_{0.5}$)HfO_3 lead-free piezoceramics were prepared by conventional sintering method, and effects of BKH on phase transition and piezoelectric properties of the ceramics are systematically investigated. XRD as well as TEM analysis indicates rhombohedral, orthorhombic and tetragonal phase coexistence for $0.03 \leq x \leq 0.05$ and greatly enhanced piezoelectric properties are observed in the ceramics with mixed phase coexistence regime, i.e., d^*_{33} (~614pm/V) and d_{33} (~400 pC/N) for x=0.035. The results show that KNNS-xBKH ceramics have potential to partially substitute PZT, and demonstrate polymorphic phase boundary (PPB) involving R phase induced by composition tuning is mostly contributed to remarkably enhanced properties of KNN-based ceramics because of lower anisotropic energy than in O-T phase coexistence PPB.

* Corresponding author: Email: mse237@zju.edu.cn

RSC Advances Accepted Manuscript

1. Introduction

As well known, the most widely used piezoelectric ceramics are the family of lead zirconate titanate [Pb(Zr,Ti) O_3, PZT] piezoceramics, which play a dominant role in practical applications of actuators, surface acoustic wave, transducers filters, and sensors, owing to their excellent function of realizing the transformation between electrical and mechanical energy.[1] However, Pb element of which the content is more than half of all in PZT piezoceramics causes terrible damage to our health as well as environment, and considerable concerns of sustainable development reasonably have made lead-free piezoceramics researches flourish recently. Due to superior piezoelectric performances and relatively high Curie temperature compared to other lead-free categories like sodium bismuth titanate ($Bi_{0.5}Na_{0.5}TiO_3$, BNT) and barium titanate ($BaTiO_3$, BT) piezoceramics, alkali niobates (K,Na)NbO_3 (KNN) lead-free piezoceramics are regarded as very promising candidates for PZT. Especially, in 2004, Saito *et al.* reported that alkaline niobates ceramics based on Li, Ta, and Sb-modified KNN show a giant d_{33} by the reactive-templated grain growth (RTGG),[2] and then it greatly encourages most researchers to highly focus on the family of KNN-based ceramics. But there is still a long way to go for practical applications regarding KNN-based ceramics, although a great of achievements have been made currently. So how to improve comprehensive properties of KNN-based ceramics is of great importance and has attracted more and more attention. Methods to solve the issue mainly include two kinds, i.e., chemical modification through doping ions as well as adding end members, and the utilization of advanced synthesis technologies. Effects

RSC Advances Accepted Manuscript

of the later on properties enhancement of KNN-based ceramics are limited, and it costs highly.[3-6] Therefore, chemical modification is more attractive and effective, and a great of attention have been paid to it lately.[7-11] Nevertheless, the properties of KNN-based ceramics are sensitive to the stoichiometry and tiny change in the composition can bring out large variations of piezoelectric properties. Additionally, how to estimate which kinds of ions can work as expected or not, is also very complicated. So chemical modification of KNN-based ceramics through composition tuning needs reasonable considerations. Previous reported researches on chemical modification of KNN-based ceramics have demonstrated the realization of polymorphic phase transition (PPT) between orthorhombic (O) and tetragonal (T) phase around room temperature (RT) through decreasing phase transition temperature of O and T phase ($T_{O\text{-}R}$) is of great validity,[4, 12, 13] but the contribution of O-T phase boundary to enhanced properties isn't remarkable, and recently a new phase boundary between rhombohedral (R) and tetragonal (T) phase has been detected in some KNN-based lead-free ceramics via adding new ABO_3-type perovskite components, which is solidly confirmed to be more available to attain much better piezoelectric properties than those of KNN-based ones owning to R, O, T phase or O-T phase coexistence boundary.[14-17]

Therefore, in order to realize the goal to improve properties of KNN-based lead-free ceramics to a larger degree, BNT-type ceramics which have been well studied as the

RSC Advances Accepted Manuscript

additions to induce R-T phase boundary in KNN,[16, 18, 19] are chosen to be the end-member of KNN ceramics, but different from previously reported researches, Hf is used to wholly substitute for Ti or Zr to form perovskite structure. In the case that quadrivalent Ti or Zr ions are responsible for spontaneous polarization and enhanced piezoelectric properties of the ceramics with perovskite structure, as they universally do in PZT and BT,[20, 21] Hf which belongs to the same ⅣB in periodic table like Ti and Zr, and possesses similar electronic figuration of $6s^2$ as well as slightly bigger ionic diameter, can also be expected to form stable solid solution with uniform perovskite structure and consequently facilitate property enhancements.[22-25]

In view of above, $(1-x)(K_{0.40}Na_{0.60})(Nb_{0.95}Sb_{0.05})O_3$-$x(Bi_{0.5}K_{0.5})HfO_3$ (KNNS-xBKH) were determined to be our research objects in this work, and effects of BKH on phase transition and piezoelectric properties of the ceramics were systematically studied. Significant improvement of d_{33}~400 pC/N and d^*_{33}~614 pm/V is acquired when x=0.035, showing that adding optimum BKH is an effective way to prompt piezoelectric properties of KNN-based ceramics, and the family of KNNS-xBKH lead-free piezoelectric ceramics have great potential to partially substitute PZT. Besides, the results suggest polymorphic phase boundary (PPB) involving R phase induced by composition tuning is mostly contributed to enhanced properties of KNN-based ceramics.

2. Experimental section

RSC Advances Accepted Manuscript

The $(1-x)(K_{0.40}Na_{0.60})(Nb_{0.95}Sb_{0.05})O_3$-$x(Bi_{0.5}K_{0.5})HfO_3$ (KNNS-xBKH) lead-free piezoceramics (x=0, 0.01, 0.02, 0.03, 0.035, 0.04, 0.045, 0.05, and 0.06) were prepared by the conventional solid-state reaction method. K_2CO_3 (99%), Na_2CO_3 (99.5%), Nb_2O_5 (99.5%), Bi_2O_3 (99%), Sb_2O_3 (99.99%), and HfO_2 (99%) were used as starting raw materials. These weighed powders were ball-milled in a polyethylene jar using ZrO_2 balls and the anhydrous ethanol for 24 h, and calcined at 850 ℃ for 6 h after drying. Calcined powders were ball milled again for 12 h and after drying, pressed into the disk pellets of 10 mm diameter and 1 mm thickness under 8 MPa. Green pellets were sintered in air at 1060~1090 ℃ for 2 h. Silver paste was coated on both sides of the samples and fired at 700 ℃ for 10 min as electrodes for measurements of electrical properties. For piezoelectric measurements, the sintered samples were poled in the silicone oil at room temperature by applying a *dc* field of 4 kV/mm for 20 min.

The crystal structure of sintered samples was characterized by the X-ray diffraction analysis (XRD, EMPYREAN, PANalytical Co., Netherlands) with Cu$K\alpha$ radiation, their surface microstructure was measured by the scanning electron microscopy (FESEM; S4800, Hitachi, Ltd., Japan), and TEM analysis was conducted for x=0.035 (TEM, Tecnai G2 F20 S-TWIN, FEI, USA). The temperature dependence of the dielectric constant (ε_r-T) was investigated by a programmable furnace in connection with an *LCR* analyses (HP4980, Agilent, USA). Their dielectric properties (ε_r) were observed by the Agilent 4294A precision impedance analyzer at the room temperature, and their piezoelectric constant (d_{33}) and the electromechanical coupling coefficients

RSC Advances Accepted Manuscript

(k_p) were measured using a piezo-d_{33} meter (Channel Product DT-3300) and impedance analyzer (Agilent 4294A), respectively. Their polarization against electric field (*P*-*E*) hysteresis loops were conducted using a standardized ferroelectric test system at room temperature and a frequency of 10 Hz. The strains that developed under the applied electric fields at 10 Hz and room temperature were examined with a MTI-2000 fotonic sensor.

3. Results and discussions

As can be seen from the characteristics of XRD patterns in Fig. 1(a), the ceramics with pure perovskite structure are obtained for $0 \leq x \leq 0.06$, suggesting BKH completely diffuses into KNNS lattice and uniform pervoskite-type solid solution of KNNS-*x*BKH ceramics forms. Furthermore, phase transition happens for $0.03 \leq x \leq 0.05$ according to split (200) peak between 45 ° and 46.5 °, as shown in Fig. 1(b). The ceramics with $0.03 \leq x \leq 0.05$ exhibit similar split characteristics of (200) peak, indicating a mixed phase coexistence in the regime. In order to discriminate phase structure, (200) peak for $x=0.035$ which is regarded to be a representative of mixed phases coexistence is simulated in Fig. 2, and it is clearly to see (200) peak split into three characterized peaks of T, O, and R phase, i.e., (200) and (020) for O phase, and (002) and (200) for T phase,[26] demonstrating R-O-T phase coexistence. The results can be generalized for $0.03 \leq x \leq 0.05$, for which (200) peaks exhibit similar shape. Different from most of previous reports on KNN-based ceramics with O-T phase

RSC Advances Accepted Manuscript

coexistence,[4, 12, 13] polymorphic phase boundary (PPB) in the work is involving R phase, and with the purpose of further examining R phase, high resolution electron microscopy (HR-TEM) measurement is conducted for x=0.035. Only a one-dimension lattice is observed in HR-TEM image of Fig. 3(a), suggesting monocrystal structure in the examination area and the most probable reason is grain size is too large to be fully detected. The insets of Fig. 3(b) and (c) are the magnification of selected area denoted in green dashed box and their fast Fourier transform (FFT), respectively. From Fig. 3(b), we obtain lattice constant d of 4.08 Å, consistent with (211) of bcc. Its fast Fourier transform (FFT) was conducted in 3(c), and corresponding diffraction spots are indexed to characteristic planes of rhombohedral phase, and therefore, R phase is determined. All indexed planes of HR-TEM and FFT strongly prove R phase exists in the ceramics with x=0.035, further verifying previous XRD analysis and simulated results. These results suggest that R-O-T phase boundary is successfully achieved for $0.03 \leq x \leq 0.05$, agreeing with the discussion of temperature-dependent dielectric constants of the ceramics measured at different temperature range later.

As well known, phase diagram of KNN-based ceramics is wholly different from PZT-based ceramics, i.e., there has no near-vertical phase boundary in KNN-based ceramics and polymorphic phase transition (PPT) is not only composition-driven but also temperature-dependent, which leads to properties instability with temperature variation.[27-29] The probable reason for PPT resulting from composition tuning is

RSC Advances Accepted Manuscript

lattice deformation through doping the ions with different radius. With respect to KNNS-*x*BKH, because the space of A and B sites enlarges due to the substitutions of larger $(Bi,K)^{2+}$ and Hf^{4+} for $(K,Na)^{+}$ and Nb^{5+}, and results in lattice expansion, as shown in Fig. 4. Besides, lattice expansion in A site induced by the impurities which lies in (001) plane, is less restricted by coordinated ions compared with the one in the center of oxygen octahedral, so the lattice is primarily stretched along [001] direction in (001) plane and phase structure reasonably turns into O phase. As a result, KNNS-*x*BKH ceramics exhibit R-O-T phase coexistence for $0.03 \leq x \leq 0.05$. In addition, because radius ratio of A site and B site is bigger than in PZT, lattice structure of KNN-based ceramics is much loose and the restriction to lattice expansion decreases compared with PZT, so phase structure of KNN-based ceramics is susceptive to tiny change of dopants, in other word, mixed phase structure coexistence regime is commonly narrower than in PZT. The loose R phase structure is also the reason why the Curie temperature decreases with *x* increasing, as discussed later. In conclusion, R phase can be induced by lattice expanding or compressing through the incorporation of the ions with proper radiuses, but in view of properties enhancement, the other factors, such as electron structure, should be taken in consideration.

Fig. 5 is surface morphologies of KNNS-*x*BKH ceramics with different *x*. All studied samples possess dense microstructure. However, anomalous grain growth with the increase of *x* is obviously detected. The results suggest that BKH significantly

RSC Advances Accepted Manuscript

facilitate grain growths. Larger grain is in favor of piezoelectric properties enhancement because the motion of domain wall can be released more compared with small grain.[30-32] On the other hand, too much larger grains can deteriorate piezoelectric properties inversely, because of much more bubbles are generated during the process of grain excessively growing, and therefore the densification of the ceramics reduces.

Temperature dependence of dielectric constant of KNNS-***x***BKH ceramics measured at different temperatures range is shown in Fig. 6. The ε_r-T plot for x=0.06 broadens obviously, showing the general features of relaxation ferroelectrics in Fig. 6(a). Besides, so as to more clearly observe phase transition activity of KNNS-xBKH, phase transition temperature as a function of x is plotted in the inset of Fig. 6(a). It can be clearly seen that $T_{O\text{-}T}$ and $T_{R\text{-}O\text{-}T}$ decreases with x increasing, and only one phase transition temperature happens for $0.03 \leq x \leq 0.05$ at low temperature, resulting from phase transition temperature of R-O phase（$T_{R\text{-}O}$）combining with $T_{O\text{-}T}$ while $T_{O\text{-}T}$ for x=0.01 or 0.02 shifts downwards to around RT, as demonstrated by previous analysis of mixed phases coexistence. Transition temperature of ferroelectric-paraferroelectric phase (T_C) for x=0.02, 0.035, 0.045, 0.06 is also observed in Fig. 6(b), and T_C decreases with x increasing. Besides, relaxation behavior for x=0.06 is investigated in the set of Fig. 6(b) as well, in which the ε_r-T plot broadens and shifts slightly to higher temperatures as the frequency increases. The reason for the declination of T_C is

RSC Advances Accepted Manuscript

closely related to easier domain wall motion stimulated by heat field due to low anisotropy energy between mixed phases and original C phase in R-O-T phase coexistence regime. Lastly, vanishing anisotropy energy between R-C phase leads to the ceramics with x=0.06 which only possess R phase experiencing the spread of ferroelectric-paraelectric phase transition over a rather wide temperature range, corresponding to broadening ε_r-T plot. Furthermore, vanishing anisotropy energy between R-C phase leads to polarization nanoregions (PNRs) arising from electric field fluctuation (RFs) induced by composition when the temperature is far above T_C, which take the most responsible for relaxor behavior of x=0.06, and decreasing temperature facilitates the nucleation of PNRs. As a result, low anisotropy energy not only makes T_C decrease in R-O-T phase coexistence regime for $0.03 \leq x \leq 0.05$, but also results in diffused phase transition (DPT) between R-C phase for x=0.06.[33, 34] Polymorphic phase transition (PPT) is confirmed to be helpful for the enhanced piezoelectric properties of KNN-based ceramics,[4, 12, 13] and in particular, dramatic properties enhancement is obtained in R-T/R-O-T phase coexistence region,[14-17] also demonstrated by optimum piezoelectric properties of KNNS- xBKH for x=0.03 and x=0.035, as shown later.

In Fig. 7(a), all samples of KNNS-xBKH exhibit saturated ferroelectric hysteresis loops, demonstrating KNNS-xBKH to be good ferroelectrics. Notably, slim P-E loop for x=0.06 is ascribed to vanishing anisotropy energy. Fig. 7(b) gives P_r and E_c as a function of x, the effects of BKH on ferroelectricity of the ceramics are to reduce both

RSC Advances Accepted Manuscript

of them to varying degree as compared with a pure KNN, and they are consequences of easier orientation of non-180° domain wall under external filed due to lower energy[35] between different phases. Furthermore, reduced E_c is helpful for sufficiently artificial poling and also results in enhanced piezoelectric properties. In a word, good ferroelectricity partially contributes to piezoelectric properties enhancement of KNNS-xBKH ceramics.

The unipolar electric field-induced strain (%) of the ceramics with different x is shown in Fig. 8. The shape of S-E loops reflects hysteretic behavior of the ceramics, and converse piezoelectric constant d^*_{33} is calculated by the slope of the loops, i.e., S_{max}/E_{max}. In Fig. 8(a), nearly linear strain of 0.14%-0.26% can be obtained at ~40 kV/cm while x increases from 0.01 to 0.05, and especially, the strain for x=0.035 increase by ~60% compared to the one for x=0.01, suggesting the non-180° domain orientation is improved remarkably under unipolar electric field due to vanishing anisotropy energy in R-O-T phase boundary. Slim S-E loops which represent degenerated hysteretic behavior resulting from the declination of non-180° domain reorientation are investigated in Fig. 8(a), and $\Delta s/s$ is used to estimate the hysteresis, in which Δs is the width of the widest part of the loop and s is the largest strain at high electric field, as shown in the inset as a function of x. As well known, degenerated hysteretic behavior as well as high strain makes ceramics especially favor of the actuator. Notably, the strain for x=0.01 is nearly equal with the one for x=0.02, and

RSC Advances Accepted Manuscript

similar phenomenon can be observed in the ceramics with x=0.04 and 0.05, suggesting that the two groups of KNNS-xBKH ceramics have similar ability of non-180° domain orientation under external field, shown in the inset of Fig. 8(b). Combining with the variation of d^*_{33} with x changing in Fig. 8(b), it can be easily concluded that non-180° domain orientation is key factor to influence d^*_{33} of KNNS-xBKH ceramics, because the two groups with similar ability of non-180° domain orientation consequently possess nearly the same d^*_{33}, respectively. Furthermore, the maximums of d^*_{33} (~614 pm/V) and d_{33} (~400 pC/N) simultaneously are acquired for x=0.035 with the largest strain, which structure lies in R-O-T phase coexistence region, illustrating the large linear strain resulting from mixed phases coexistence induced by the incorporation of BKH is extremely responsible for large piezoelectric response.

Piezoelectric properties of KNNS-xBKH ceramics as a function of x is presented in Fig. 9. It can be clearly seen d_{33} increases firstly, then begins to gradually decrease as x further increasing, and reaches its maximum of ~400 pC/N at x=0.035. The values of d_{33} of KNNS-xBKH ceramics are higher than those of pure KNNS (~120 pC/N), showing appropriate BKH benefits enhanced piezoelectric properties of KNNS-xBKH. More about the degree to which piezoelectric properties are enhanced, can be investigated in Fig. 9(b) concerning the amplification of d_{33} calculate by the ratio of d_{33} for the others to the one for x=0.01. Obviously, the ceramics with $0.03 \leq x \leq 0.045$

RSC Advances Accepted Manuscript

which structures lie in R-O-T coexistence phase boundary around RT, have much larger d_{33} than the ceramics with x=0.02 which possess O phase only, and impressively, the amplification for x=0.03 or x=0.035 are on the order of ~100%. The results show that the construction of R-O-T phase boundary is mostly contributed to great enhancement of piezoelectric properties of KNN-based ceramics, and appropriate BKH is an effective addition to construct R-O-T phase boundary. Different from d_{33}, k_p changes slightly for $0.01 \leq x \leq 0.45$ with the change of x, except k_p of ~ 0.28 for x=0.05. The reasons for enhanced piezoelectric properties can be explained that R-O-T phase coexistence for $0.03 \leq x \leq 0.045$ generates more possible polarization states and the motion of domain wall becomes easier due to lower anisotropy energy among these mixed phases,[1, 36, 37] both of them resulting in more sufficient polarization orientation through artificial poling. Nevertheless, the ceramics with x=0.05 which also lie in R-O-T phase boundary behave in a different fashion, and the reason is illustrated later.

In order to clearly identify what mainly influences piezoelectric properties enhancement of KNNS-xBKH, the comparison of *P*-*E* loops and *S*-*E* loops for two group ceramics with different x is presented in Figs. 10(a), (b), (c) and (d). As mentioned before, the ceramics for x=0.01 and 0.02 have nearly the same remnant polarization (P_r), and the result is also observed for x=0.04 and 0.05 in Fig. 10(b). Strain (%) variations of two group ceramics under high electric field are also similar,

RSC Advances Accepted Manuscript

as shown in Figs. 10(c) and (d). As well known, main contributions to piezoelectric properties are spontaneous polarizations as well as their orientation, and domain wall motion. The results of P_r and strain comparison between x=0.01 and 0.02, or x=0.04 and 0.05 suggest that the effect of spontaneous polarizations and their orientation under external field is nearly equal in the two groups. But piezoelectric properties in the two groups are not the same but obviously variable, indicating phase boundary migration owing to domain wall motion takes primary responsibility for large piezoelectric response, which is also affected by two factors, i.e., the energy and pinning effect. As far as the energy is concerned, domain wall motion is easier in polymorphic phases coexistence than in sole ferroelectric phase due to lower anisotropy energy among mixed phases, and especially, the contribution of PPB involving R phase to lowering anisotropy energy is of more importance, because the energy decreases while θ reducing, as presented in Fig. 10(e). This is the main reason why piezoelectric properties for $0.03 \leq x \leq 0.045$ in R-O-T phase boundary are much higher than those for x=0.01 and 0.02 in O-T phase boundary in Fig. 9(b). Exceptionally, piezoelectric properties for x=0.05 degenerate inversely, which is defined as the margin of R-O-T phase coexistence regime, and the cause of the most probability is strengthened pinning effect owing to excess addition of BKH. Nonequivalence of $(Bi, K)^{2+}$ and Hf^{4+} partially substitute for $(K, Na)^{+}$ and $(Nb, Sb)^{5+}$, giving rise to equal cation vacancies (V_C') and oxygen ion vacancies ($V_O^{\cdot\cdot}$) simultaneously, as shown in following formula: $(Bi, K)^{2+} + Hf^{4+} \rightarrow (K, Na)^{+} + (Nb,$

RSC Advances Accepted Manuscript

Sb)$^{5+}$ + V_C' + 1/2$V_O^{\cdot\cdot}$, these defects created by the impurities function together and influence domain wall motion, and the more x is, the more remarkable the contribution of pinning centers to domain motion becomes.[38, 39] Consequently, when x=0.05, domain wall motion is severely hindered, resulting in piezoelectric properties anomalously decreasing. But this pinning effect works only for a particular range of temperatures, and valid method to decrease the effect as well as increase the level of domain wall motion is preventing the diffusion of these defects through thermal quenching from far above T_C.[40, 41] The schematic diagrams of domain wall motion are shown in Fig. 10(f).

In order to learn more about the depolarization behavior of KNNS-xBKH, composition-dependent d_{33}^0/d_{33}^T as a function of the temperature is observed in Fig. 11, where d_{33}^0 is piezoelectric constant at room temperature and d_{33}^T is the ones at different depolarization temperature. As we can see, d_{33}^0/d_{33}^T changes gently until over 200°C for 0.01≤x≤0.035, and variation rate of piezoelectric constant keeps within the limit of ~10%. With further increasing x, the decrease of piezoelectric constant with temperature variation becomes steeper, suggesting that temperature stability degenerates. In general, KNNS-xBKH ceramics with x=0.035 possess optimum properties and good depolarization behavior as the temperature rises, and are promising substitutes for lead-free ceramics in some actual application.

RSC Advances Accepted Manuscript

4. Conclusion

$(1-x)(K_{0.40}Na_{0.60})(Nb_{0.95}Sb_{0.05})O_3$-$x(Bi_{0.5}K_{0.5})HfO_3$ (KNNS-xBKH) piezoceramics are well prepared by conventional sintering method, and phase structure as well as piezoelectric properties are systematically studied. Significantly enhanced properties are obtained for $0.03 \leq x \leq 0.045$, which structures locate in R-O-T phase coexistence regime. In particular, the ceramics with x=0.035 possess the best piezoelectric properties (i.e., d^*_{33}~614 pm/V and d_{33}~400 pC/N) and good depolarization behavior, suggesting to be promising candidates for PZT in some application. Above all, the results demonstrate polymorphic phase boundary (PPB) involving R phase induced by composition tuning is mostly contributed to dramatically enhanced properties of KNN-based ceramics because of lower anisotropic energy than in O-T phase coexistence PPB.

Author information

Corresponding author

*E-mail address: mse237@zju.edu.cn (Q. Zhang).

Present address

School of Materials Science and Engineering, State Key Lab Silicon Mat, Zhejiang University, Hangzhou 310027, PR China

Acknowledgements

The authors gratefully acknowledge the financial support from the National High

RSC Advances Accepted Manuscript

Technology Research and Development Program of China (863 Program) (No. 2013AA030701) and the Fundamental Research Funds for the Central Universities (No. 2015QNA4007).

RSC Advances Accepted Manuscript

References:

1 B. Jaffe, R. S. Roth, S. Marzullo, "Properties of Piezoelectric Ceramics in the Solid-Solution Series Lead Titanate-Lead Zirconate-Lead Oxide-Tin Oxide and Lead Titanate-Lead Hafnate", *J. Res. Nat. Bur. Stand.,* 1955, **55** (5), 239-254.

2 Y. Saito, H. Takao, T. Tani, T. Nonoyama, K. Takatori, T. Homma, T. Nagaya, M. Nakamura, "Lead-free piezoceramics", *Nature,* 2004, **432** (7013), 84-87.

3 J. F. Li, K. Wang, B. P. Zhang, L. M. Zhang, "Ferroelectric and piezoelectric properties of fine-grained $Na_{0.5}K_{0.5}NbO_3$ lead-free piezoelectric ceramics prepared by spark plasma sintering", *J. Am. Ceram. Soc.,* 2006, **89** (2), 706-709.

4 Y. F. Chang, S. Poterala, Z. P. Yang, G. L. Messing, "Enhanced Electromechanical Properties and Temperature Stability of Textured $(K_{0.5}Na_{0.5})NbO_3$-Based Piezoelectric Ceramics", *J. Am. Ceram. Soc.,* 2011, **94** (8), 2494-2498.

5 E. Mensur-Alkoy, A. Berksoy-Yavuz, S. Alkoy, "Processing and Properties of Textured Potassium Sodium Niobate $[K,Na]NbO_3$ Ceramic Ribbons by Alginate Gelation Method", *J. Am. Ceram. Soc.,* 2014, **97** (11), 3425-3433.

6 A. B. Haugen, G. H. Olsen, F. Madaro, M. I. Morozov, G. Tutuncu, J. L. Jones, T. Grande, M. A. Einarsrud, "Piezoelectric $K_{0.5}Na_{0.5}NbO_3$ Ceramics Textured Using Needlelike $K_{0.5}Na_{0.5}NbO_3$ Templates", *J. Am. Ceram. Soc.,* 2014, **97** (12), 3818-3825.

7 H. E. Mgbemere, M. Hinterstein, G. A. Schneider, "Investigation of the Structure and Electrical Properties of $(K_xNa_{0.96-x}Li_{0.04})(Nb_{0.96-y}Ta_ySb_{0.04})O_3$ Piezoelectric Ceramics Modified with Manganese", *J. Am. Ceram. Soc.,* 2013, **96** (1), 201-208.

RSC Advances Accepted Manuscript

8 F. Z. Yao, K. Wang, J. F. Li, "Comprehensive investigation of elastic and electrical properties of Li/Ta-modified (K,Na)NbO_3 lead-free piezoceramics", *J. Appl. Phys.,* 2013, **113** (17), 174105.

9 T. Matsuoka, H. Kozuka, K. Kitamura, H. Yamada, T. Kurahashi, M. Yamazaki, K. Ohbayashi, "KNN-NTK composite lead-free piezoelectric ceramic", *J. Appl. Phys.,* 2014, **116** (15), 154104.

10 Y. B. Wei, Z. Wu, Y. M. Jia, J. Wu, Y. C. Shen, H. S. Luo, "Dual-enhancement of ferro-/piezoelectric and photoluminescent performance in Pr^{3+} doped $(K_{0.5}Na_{0.5})NbO_3$ lead-free ceramics", *Appl. Phys. Lett.,* 2014, **105** (4), 042902.

11 S. M. Ke, H. T. Huang, H. Q. Fan, H. K. Lee, L. M. Zhou, Y. W. Mai, "Antiferroelectric-like properties and enhanced polarization of Cu-doped $K_{0.5}Na_{0.5}NbO_3$ piezoelectric ceramics", *Appl. Phys. Lett.,* 2012, **101** (8), 082901.

12 S. J. Zhang, R. Xia, T. R. Shrout, "Modified $(K_{0.5}Na_{0.5})NbO_3$ based lead-free piezoelectrics with broad temperature usage range", *Appl. Phys. Lett.,* 2007, **91** (13), 132913.

13 S. J. Zhang, R. Xia, T. R. Shrout, G. Z. Zang, J. F. Wang, "Piezoelectric properties in perovskite $0.948(K_{0.5}Na_{0.5})NbO_3$-$0.052LiSbO_3$ lead-free ceramics", *J. Appl. Phys.,* 2006, **100** (10), 104108.

14 J. G. Wu, H. Tao, Y. Yuan, X. Lv, X. J. Wang, X. J. Lou, "Role of antimony in the phase structure and electrical properties of potassium-sodium niobate lead-free ceramics", *Rsc Adv.,* 2015, **5** (19), 14575-14583.

RSC Advances Accepted Manuscript

15 Z. Wang, D. Q. Xiao, J. G. Wu, M. Xiao, F. X. Li, J. G. Zhu, "New Lead-Free (1 - x)($K_{0.5}Na_{0.5}$) NbO_3-x($Bi_{0.5}Na_{0.5}$)ZrO_3 Ceramics with High Piezoelectricity", *J. Am. Ceram. Soc.,* 2014, **97** (3), 688-690.

16 X. J. Cheng, J. G. Wu, X. P. Wang, B. Y. Zhang, J. G. Zhu, D. Q. Xiao, X. J. Wang, X. J. Lou, W. F. Liang, "Lead-free piezoelectric ceramics based on (0.97-x)$K_{0.48}Na_{0.52}NbO_3$-0.03$Bi_{0.5}(Na_{0.7}K_{0.2}Li_{0.1})_{0.5}ZrO_3$-$xBi_{0.5}Na_{0.5}TiO_3$ ternary system", *J. Appl. Phys.,* 2013, **114** (12), 124107.

17 J. Wu, D. Xiao, J. Zhu, "Potassium–Sodium Niobate Lead-Free Piezoelectric Materials: Past, Present, and Future of Phase Boundaries", *Chem. Rev.,* 2015, 2559-2595.

18 Y. Hiruma, K. Yoshii, H. Nagata, T. Takenaka, "Phase transition temperature and electrical properties of $(Bi_{1/2}Na_{1/2})TiO_3$-$(Bi_{1/2}A_{1/2})TiO_3$ (A=Li and K) lead-free ferroelectric ceramics", *J. Appl. Phys.,* 2008, **103** (8), 084121.

19 X. J. Cheng, J. G. Wu, X. P. Wang, B. Y. Zhang, J. G. Zhu, D. Q. Xiao, X. J. Wang, X. J. Lou, "New lead-free piezoelectric ceramics based on $(K_{0.48}Na_{0.52})(Nb_{0.95}Ta_{0.05})O_3$-$Bi_{0.5}(Na_{0.7}K_{0.2}Li_{0.1})_{0.5}ZrO_3$", *Dalton T.,* 2014, **43** (9), 3434-3442.

20 F. Rubio-Marcos, J. J. Romero, M. S. Martin-Gonzalez, J. F. Fernandez, "Effect of stoichiometry and milling processes in the synthesis and the piezoelectric properties of modified KNN nanoparticles by solid state reaction", *J. Eur. Ceram. Soc.,* 2010, **30** (13), 2763-2771.

RSC Advances Accepted Manuscript

21 F. Rubio-Marcos, P. Ochoa, J. F. Fernandez, "Sintering and properties of lead-free (K,Na,Li)(Nb,Ta,Sb)O_3 ceramics", *J. Eur. Ceram. Soc.,* 2007, **27** (13-15), 4125-4129.

22 G. Fantozzi, H. Idrissi, C. Favotto, M. Roubin, "Lead hafnate titanate (PHT) ceramics: processing and properties", *J. Eur. Ceram. Soc.,* 2000, **20** (11), 1671-1676.

23 D. L. Wang, Z. H. Jiang, B. Yang, S. T. Zhang, M. F. Zhang, F. F. Guo, W. W. Cao, "Phase transition behavior and high piezoelectric properties in lead-free $BaTiO_3$-$CaTiO_3$-$BaHfO_3$ ceramics", *J. Mater. Sci.,* 2014, **49** (1), 62-69.

24 A. Hussain, C. W. Ahn, A. Ullah, J. S. Lee, I. W. Kim, "Effects of Hafnium Substitution on Dielectric and Electromechanical Properties of Lead-free $Bi_{0.5}(Na_{0.78}K_{0.22})_{0.5}(Ti_{1-x}Hf_x)O_3$ Ceramics", *Jpn. J. Appl. Phys.,* 2010, **49** (4), 041504.

25 A. K. Kalyani, K. Brajesh, A. Senyshyn, R. Ranjan, "Orthorhombic-tetragonal phase coexistence and enhanced piezo-response at room temperature in Zr, Sn, and Hf modified $BaTiO_3$", *Appl. Phys. Lett.,* 2014, **104** (25), 252906.

26 Ke Wang and Jing-Feng Li, " Analysis of crystallographic evolution in (Na , K) NbO_3 -based lead-free piezoceramics by x-ray diffraction", *Appl. Phys. Lett*., 2007, **91**, 262902.

27 S. J. Zhang, R. Xia, T. R. Shrout, "Lead-free piezoelectric ceramics vs. PZT?", *J. Electroceram.,* 2007, **19** (4), 251-257.

28 T. R. Shrout, S. J. Zhang, "Lead-free piezoelectric ceramics: Alternatives for PZT?", *J. Electroceram.,* 2007, **19** (1), 113-126.

29 D. E. Cox, B. Noheda, G. Shirane, Y. Uesu, K. Fujishiro, Y. Yamada, "Universal

RSC Advances Accepted Manuscript

phase diagram for high-piezoelectric perovskite systems", *Appl. Phys. Lett.,* 2001, **79** (3), 400-402.

30 P. Bharathi, K. B. R. Varma, "Grain and the concomitant ferroelectric domain size dependent physical properties of $Ba_{0.85}Ca_{0.15}Zr_{0.1}Ti_{0.9}O_3$ ceramics fabricated using powders derived from oxalate precursor route", *J. Appl. Phys.,* 2014, **116** (16), 164107.

31 J. L. Zhang, P. F. Ji, Y. Q. Wu, X. Zhao, Y. Q. Tan, C. L. Wang, "Strong piezoelectricity exhibited by large-grained $BaTiO_3$ ceramics", *Appl. Phys. Lett.,* 2014, **104** (22), 222909.

32 H. Y. Ge, Y. Y. Huang, Y. D. Hou, H. Xiao, M. K. Zhu, "Size dependence of the polarization and dielectric properties of $KNbO_3$ nanoparticles", *Rsc. Adv.,* 2014, **4** (44), 23344-23350.

33 V. Bobnar, J. Holc, M. Hrovat, M. Kosec, "Relaxorlike dielectric dynamics in the lead-free $K_{0.5}Na_{0.5}NbO_3$-$SrZrO_3$ ceramic system", *J. Appl. Phys.,* 2007, **101** (7), 074103.

34 V. V. Shvartsman, D. C. Lupascu, "Lead-Free Relaxor Ferroelectrics", *J. Am. Ceram. Soc.,* 2012, **95** (1), 1-26.

35 S. Poykko, D. J. Chadi, "Ab initio study of 180 degrees domain wall energy and structure in $PbTiO_3$", *Appl. Phys. Lett.,* 1999, **75** (18), 2830-2832.

36 W. F. Liu, X. B. Ren, "Large Piezoelectric Effect in Pb-Free Ceramics", *Phys. Rev. Lett.,* 2009, **103** (25), 25760.

RSC Advances Accepted Manuscript

37 T. Zheng, J. Wu, D. Xiao, J. Zhu, X. Wang, L. Xin, X. Lou, "Strong Piezoelectricity in $(1–x)(K_{0.4}Na_{0.6})(Nb_{0.96}Sb_{0.04})O_3$-$xBi_{0.5}K_{0.5}Zr_{1-y}Sn_yO_3$ Lead-Free Binary System: Identification and Role of Multiphase Coexistence", *Acs. Appl. Mater. Inter.,* 2015, 5927-5937.

38 J. E. Garcia, D. A. Ochoa, V. Gomis, J. A. Eiras, R. Perez, "Evidence of temperature dependent domain wall dynamics in hard lead zirconate titanate piezoceramics", *J. Appl. Phys.,* 2012, **112** (1), 014113.

39 J. E. Garcia, R. Perez, D. A. Ochoa, A. Albareda, M. H. Lente, J. A. Eiras, "Evaluation of domain wall motion in lead zirconate titanate ceramics by nonlinear response measurements", *J. Appl. Phys.,* 2008, **103** (5), 054108.

40 T. Rojac, M. Kosec, B. Budic, N. Setter, D. Damjanovic, "Strong ferroelectric domain-wall pinning in $BiFeO_3$ ceramics", *J. Appl. Phys.,* 2010, **108** (7), 074107.

41 J. Nuffer, D. C. Lupascu, J. Rodel, "Stability of pinning centers in fatigued lead-zirconate-titanate", *Appl. Phys. Lett.,* 2002, **80** (6), 1049-1051.

RSC Advances Accepted Manuscript

Table I: Comparison of piezoelectric properties among different KNN-based ceramics

Properties	This work	KNNLT[8]	KNN-NTK[9]	KNN-*x*Pr[10]	KNNS[14]	KNN-*x*BNZ[15]	PZT5A[27]
d_{33} (pC/N)	**~400**	**195**	**252**	**108**	**210**	**360**	**375**
d^*_{33} (pm/V)	**~614**	**308**	**----**	**---**	**~300**	**---**	**600**
K_P	**0.40**	**0.38**	**0.52**	**0.29**	**0.45**	**0.32**	**0.71**

RSC Advances Accepted Manuscript

Figure captions

Fig. **1(a)** XRD patterns and **(b)** expanded XRD patterns (45°~46.5°) of KNNS-*x*BKH ceramics

Fig. **2** Simulated peaks of (200) characteristic peak for x=0.035

Fig. **3** HR-TEM image for x=0.035; **(a)** the magnification of selected area denoted in green dashed box; **(b)** their fast Fourier transform (FFT) and **(c)** corresponding XRD patterns of rhombohedral phase

Fig. **4** Schematic diagram of R-O-T phase coexistence induced by lattice expansion

Fig. **5** Surface morphologies of KNNS-*x*BKH ceramics with **(a)** x=0.01; **(b)** x=0.035; **(c)** x=0.045 and **(d)** x=0.06

Fig. **6** ε_r-T loops as a function of x over temperature range of **(a)** -150 ^{o}C-200 ^{o}C; **(b)** 0 ^{o}C-500 ^{o}C

Fig. **7(a)** P-E loops of KNNS-*x*BKH ceramics; **(b)** the change of P_r and E_C with the variation of x

Fig. **8(a)** Unipolar strain curves of the indicated samples and **(b)** d_{33} and d^*_{33} as a function of x

Fig. **9(a)** Piezoelectric properties of KNNS-*x*BKH ceramics as a function of x and **(b)** the amplifications of d_{33} compared with x=0.01

Fig. **10** The comparison of **(a)**, **(b)** ferroelectric properties and **(c)**, **(d)** the strains for the two groups with different x; **(e)** anisotropic energy ascribed to θ and **(f)** domain wall motion related to pinning effect.

Fig. **11** Depolarization behavior of KNNS-*x*BKH ceramics as a function of the temperature

RSC Advances Accepted Manuscript

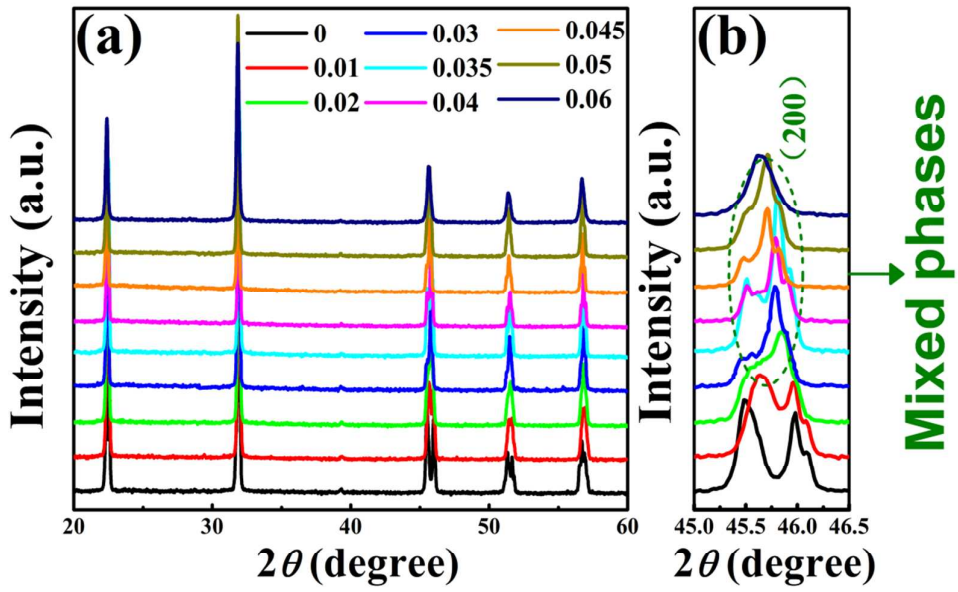

Fig. 1

RSC Advances Accepted Manuscript

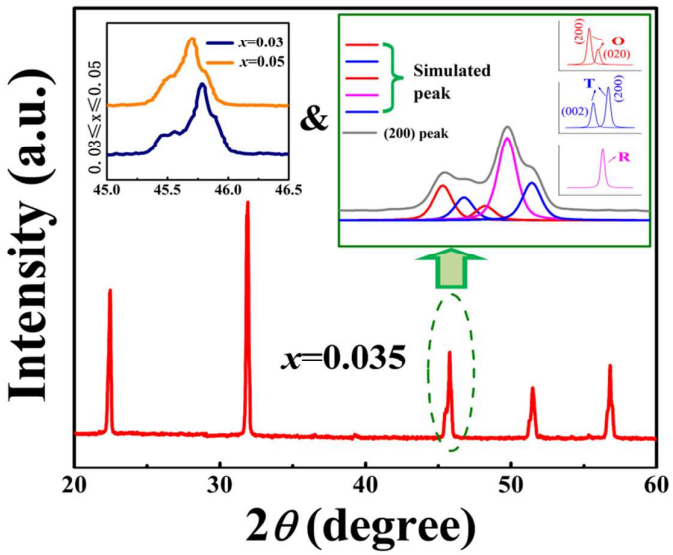

Fig. 2

RSC Advances Accepted Manuscript

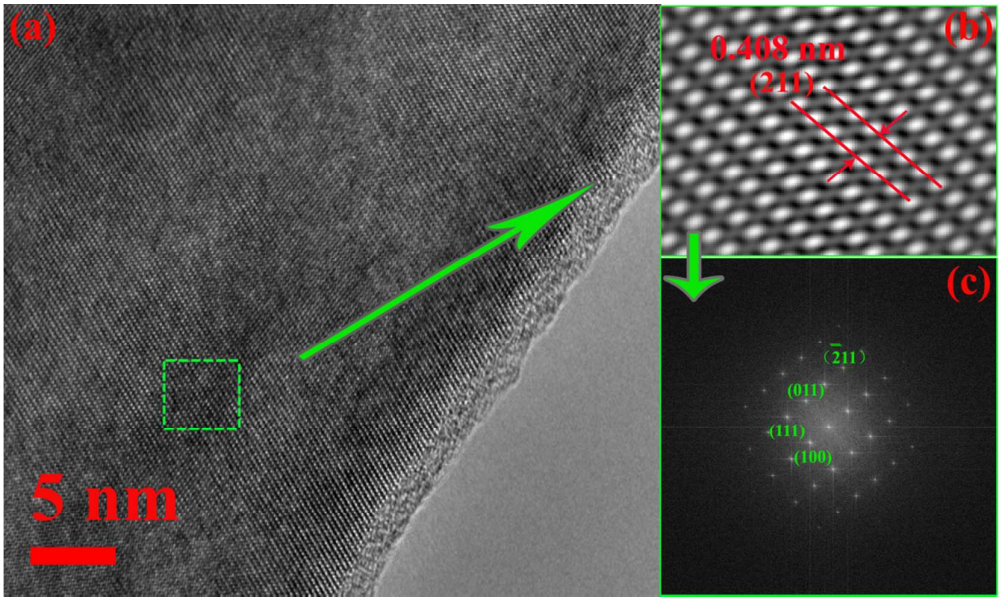

Fig. 3

RSC Advances Accepted Manuscript

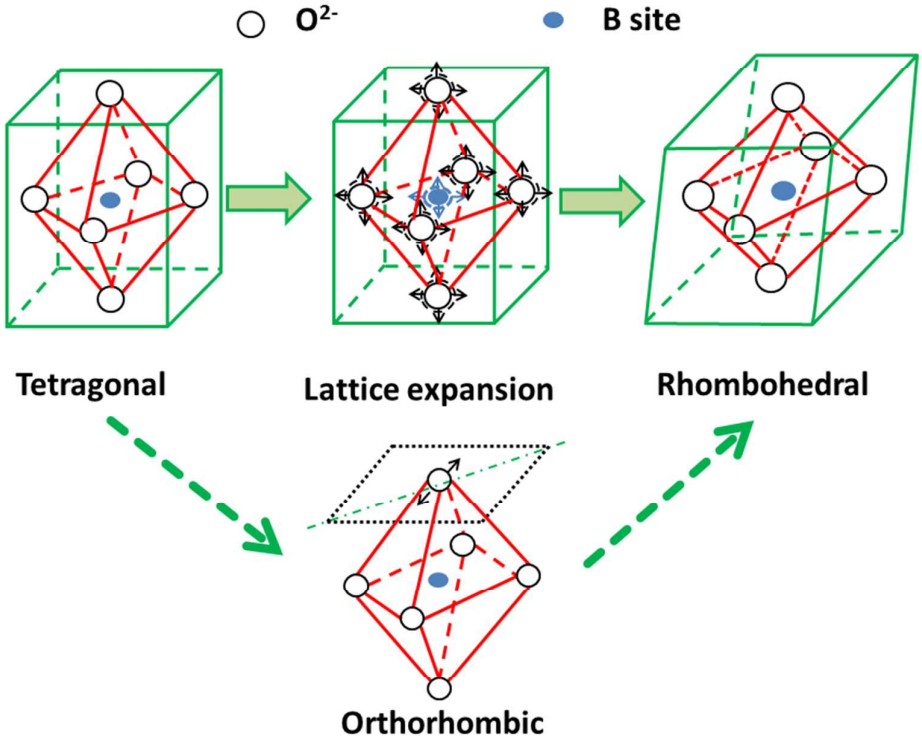

Fig. 4

RSC Advances Accepted Manuscript

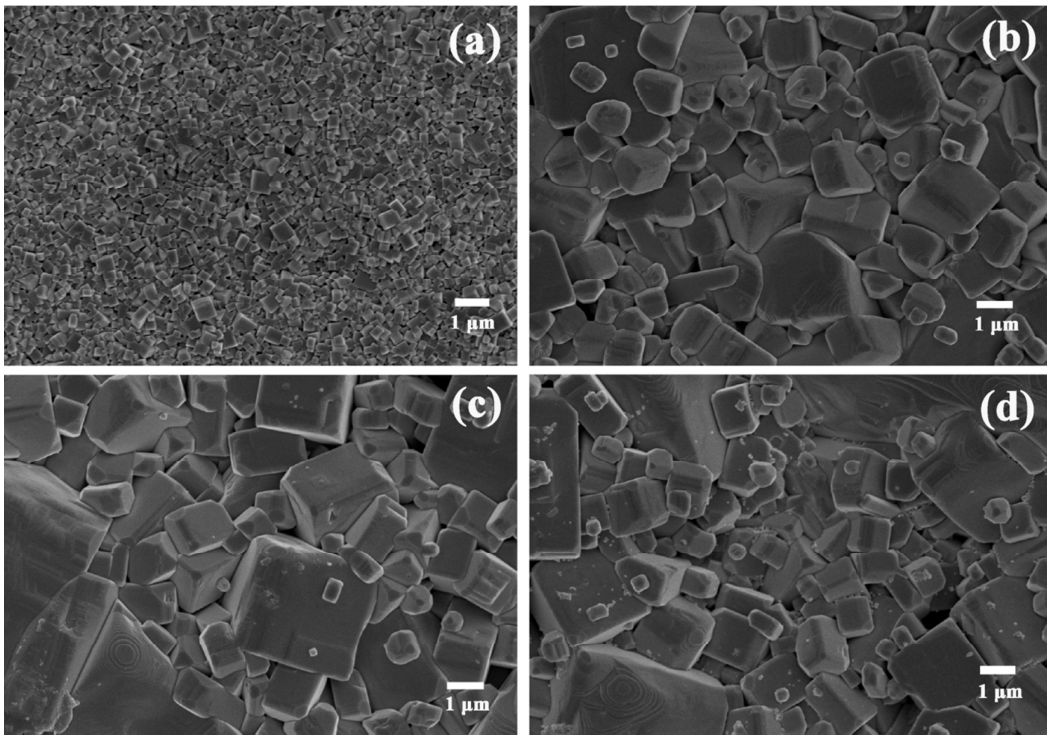

Fig. 5

RSC Advances Accepted Manuscript

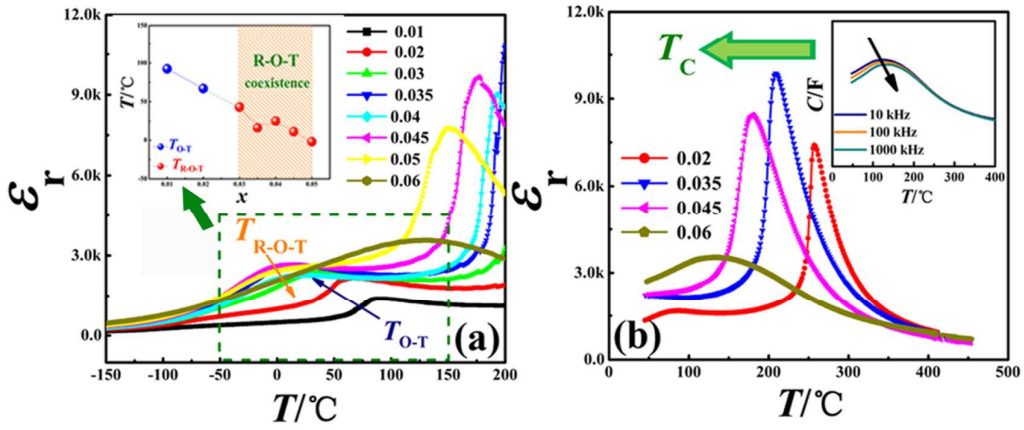

Fig. 6

RSC Advances Accepted Manuscript

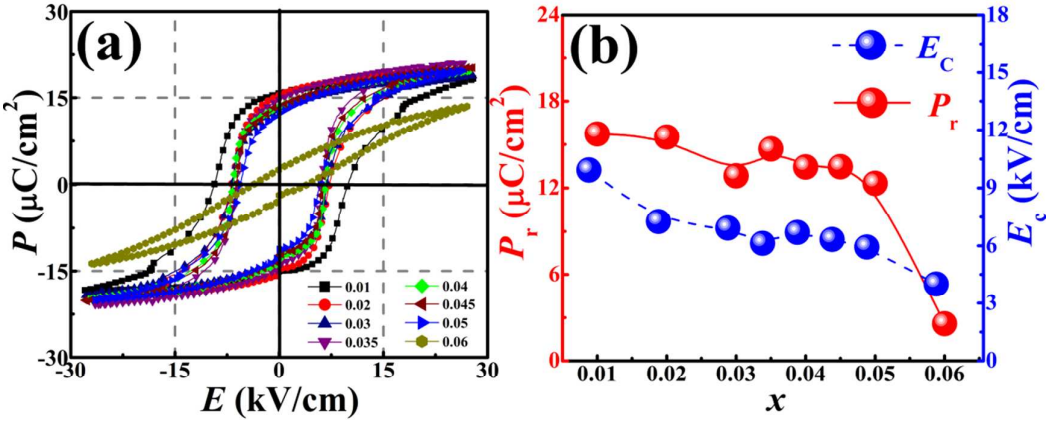

Fig. 7

RSC Advances Accepted Manuscript

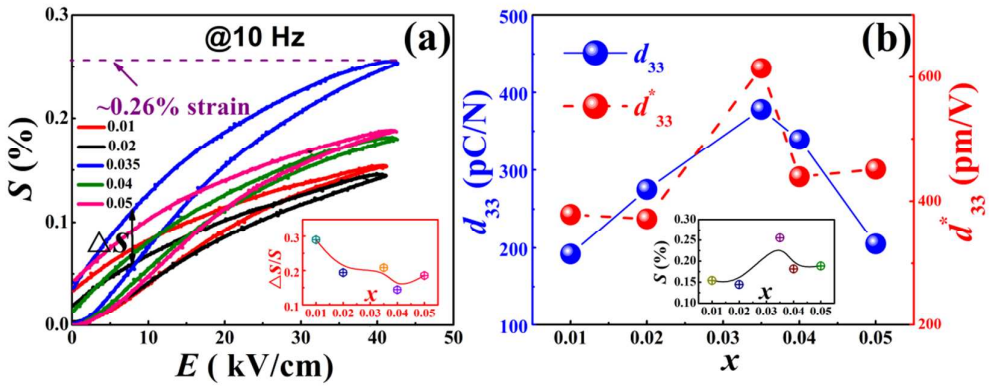

Fig. 8

RSC Advances Accepted Manuscript

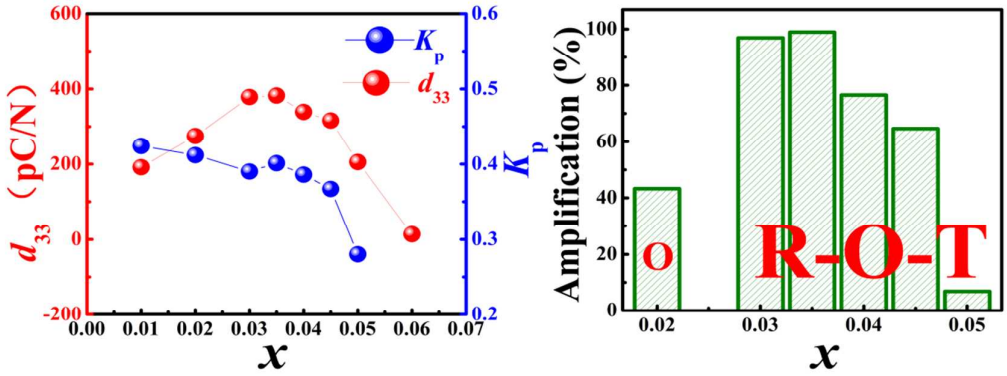

Fig. 9

RSC Advances Accepted Manuscript

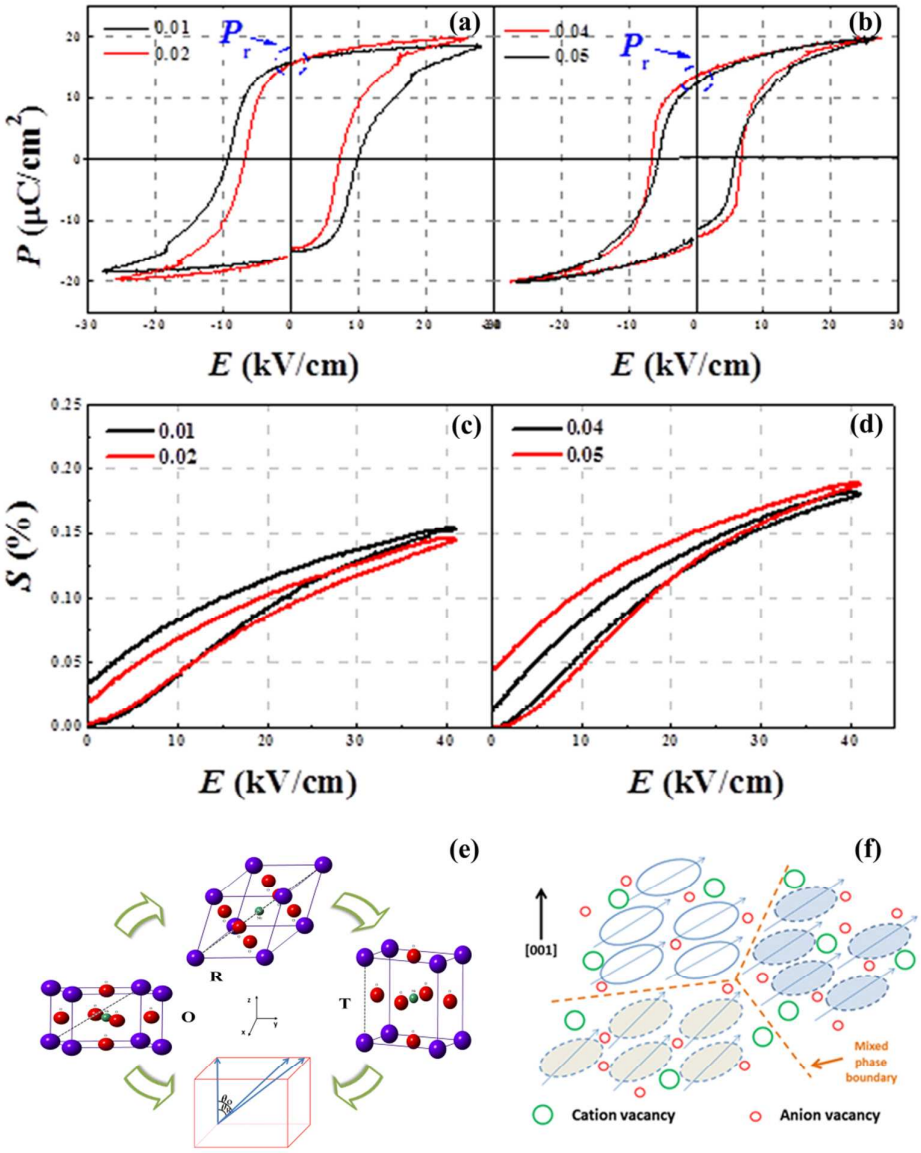

Fig. 10

RSC Advances Accepted Manuscript

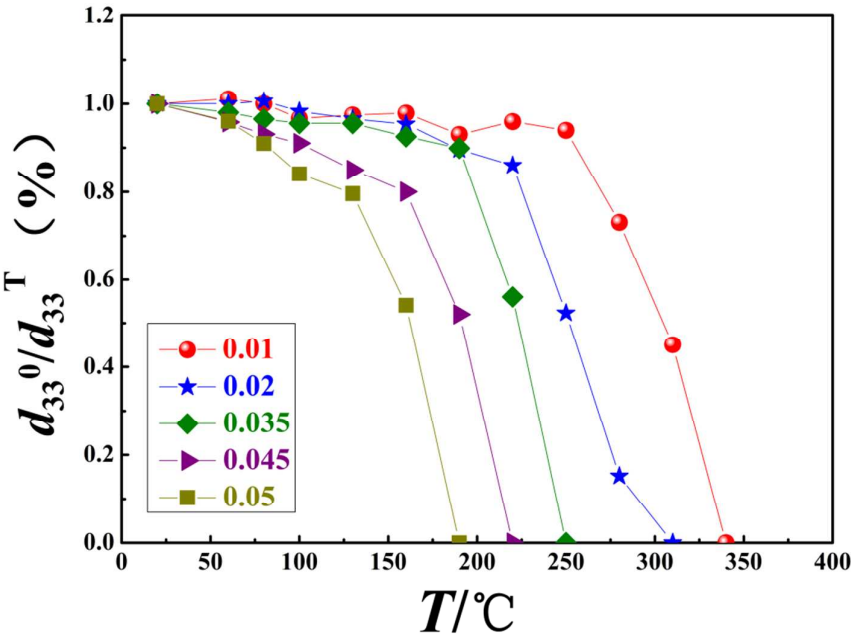

Fig. 11

RSC Advances Accepted Manuscript